

Lists of table and figure captions:

Table S1. BVS calculations of Mo and P centers in compounds **1-3**.

Table S2. BVS calculations of M centers in compounds **1-3**.

Table S3. Reduction of Cr(VI) catalyzed by compounds **1-3** at 55° C.

Fig. S1. UV-Vis spectra of Cr(VI) solution at different concentrations (from inner to outer: 0.1×10^{-4} , 1×10^{-4} , 5×10^{-4} , 8×10^{-4} , and 10×10^{-4} mol·L⁻¹); the inset is the dependence of Cr(VI) concentration and absorbance at 348 nm.

Fig. S2. (a) The polyhedral view of the sandwich type structural unit {Fe[P₄Mo₆]₂} in **1**; (b) A simplified ball-and-rod view of two {Fe[P₄Mo₆]₂} clusters is shown in **1**. Mo is shown as light blue, Fe atoms are yellow, and O, H and P atoms are ignored.; (c) Fe1-[P₄Mo₆]₂ and Fe2-[P₄Mo₆]₂ anion clusters are alternately arranged to form one-dimensional chains by hydrogen bonding.

Fig. S3. IR spectra of (a) compound **1**, (b) compound **2**, and (c) compound **3**.

Fig. S4. TG of (a) compound **1**, (b) compound **2**, and (c) compound **3**.

Fig. S5. Comparison of the simulated and experimental XRD patterns of compounds **1** (a), **2** (b) and **3** (c).

Fig. S6. EDS spectra of compounds **1-3** show the weight percentages of the elements and the total percentage of atoms. The EDS energy spectra were measured at 20 KV. The right pictures show that the compounds contain Fe, Zn, and Mn atoms. In the left Table, the atomic ratios of P:Mo:M (M = Fe/Zn/Mn) are *ca.* 4:6:1 in compounds **1-3**, and are also consistent with the structural analysis results.

Table S1. BVS calculations of Mo and P centers in compounds **1-3**.

	Compound 1	Compound 2	Compound 3
Mo1	5.219	5.332	4.881
Mo2	5.261	5.323	4.920
Mo3	5.306	5.323	5.040
Mo4	5.274	5.377	4.884
Mo5	5.268	5.297	4.968
Mo6	5.279	5.311	4.968
P1	4.820	4.943	4.639
P2	4.909	4.972	4.586
P3	4.892	4.882	4.681
P4	4.827	4.989	4.815

Table S2. BVS calculations of M centers in compounds **1-3**.

	Compound 1		Compound 2		Compound 3	
Fe1	1.874	Zn1	1.791	Mn1	2.060	
Fe2	1.857	Zn2	1.759	Mn2	1.978	

Table S3. Reduction of Cr(VI) catalyzed by compounds **1-3** at 55° C.

Compound	n(K ₂ Cr ₂ O ₇) [10 ⁻⁵ mol]	n(catalyst) [10 ⁻⁶ mol]	Conversion (%)	TON ^a	TOF ^b [10 ⁻⁴ s ⁻¹]
None	2.2	0	0	0	0
1	2.2	3.14	83.83	1.5	1.4
2	2.2	3.15	0	0	0
3	2.2	3.50	0	0	0

^aTON = (2 × mole of K₂Cr₂O₇ × conversion) / (mole of catalyst); ^bTOF = (2 × mole of K₂Cr₂O₇ × conversion) / (mole of catalyst × time). Time is 30 min.

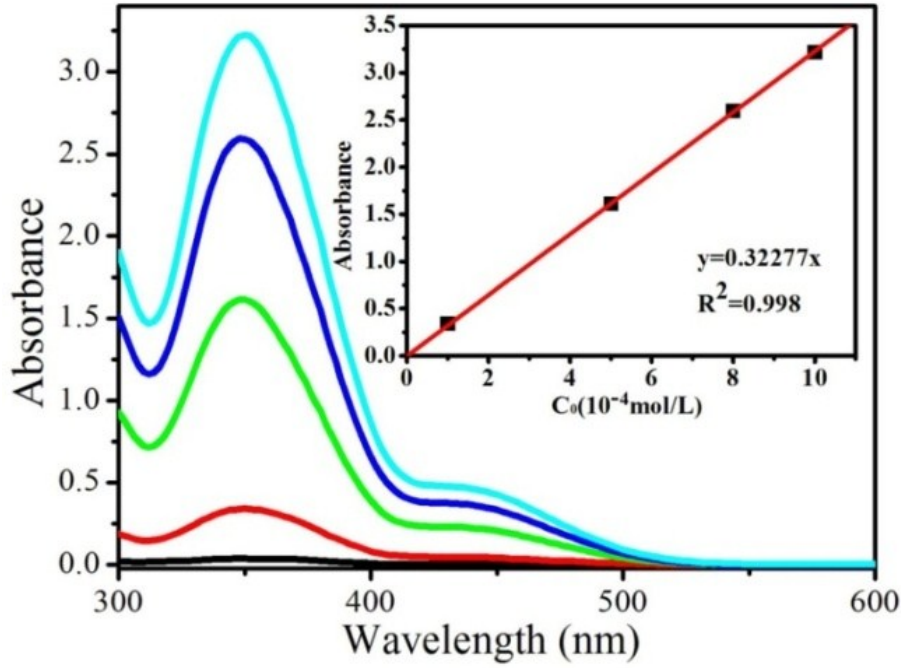


Fig. S1. UV-Vis spectra of Cr(VI) solution at different concentrations (from inner to outer: 0.1×10^{-4} , 1×10^{-4} , 5×10^{-4} , 8×10^{-4} , and 10×10^{-4} mol·L⁻¹); the inset is the dependence of Cr(VI) concentration and absorbance at 348 nm.

Concentrations were determined by absorbance. When the incident light, absorption coefficient and path length keep same, the transmitted light only changes with the concentration of the solution. So in a certain range, the C and absorbance A accord with the Lambert's law.

$$A = \kappa b C \quad (1)$$

The maximum absorption wavelength of Cr(VI) is at 346 nm. And the value is selected to obtain the relationship between the concentration of Cr(VI) and its absorbance. As shown in Fig. 1, the absorbance intensities have a good linear relationship with the concentration of Cr(VI) at the characteristic wavelength. The linear fitting equation is:

$$A = 0.32277\rho, \quad R^2 = 0.998 \quad (2)$$

In the formula: A is the absorbance value, ρ is the molar concentration of K₂Cr₂O₇. Indicating when the molar concentration is less than 1.0×10^{-3} mol·L⁻¹, the relationship of concentration and absorbance well conforms to the Lambert-Beer law. Then the percent conversion can be showed by the following formula:

$$D = (A_0 - A_t) / A_0 \times 100\% \quad (3)$$

Thereinto: D is the percent conversion, A_0 is the initial solution absorbance, A_t is the absorbance at time t min.

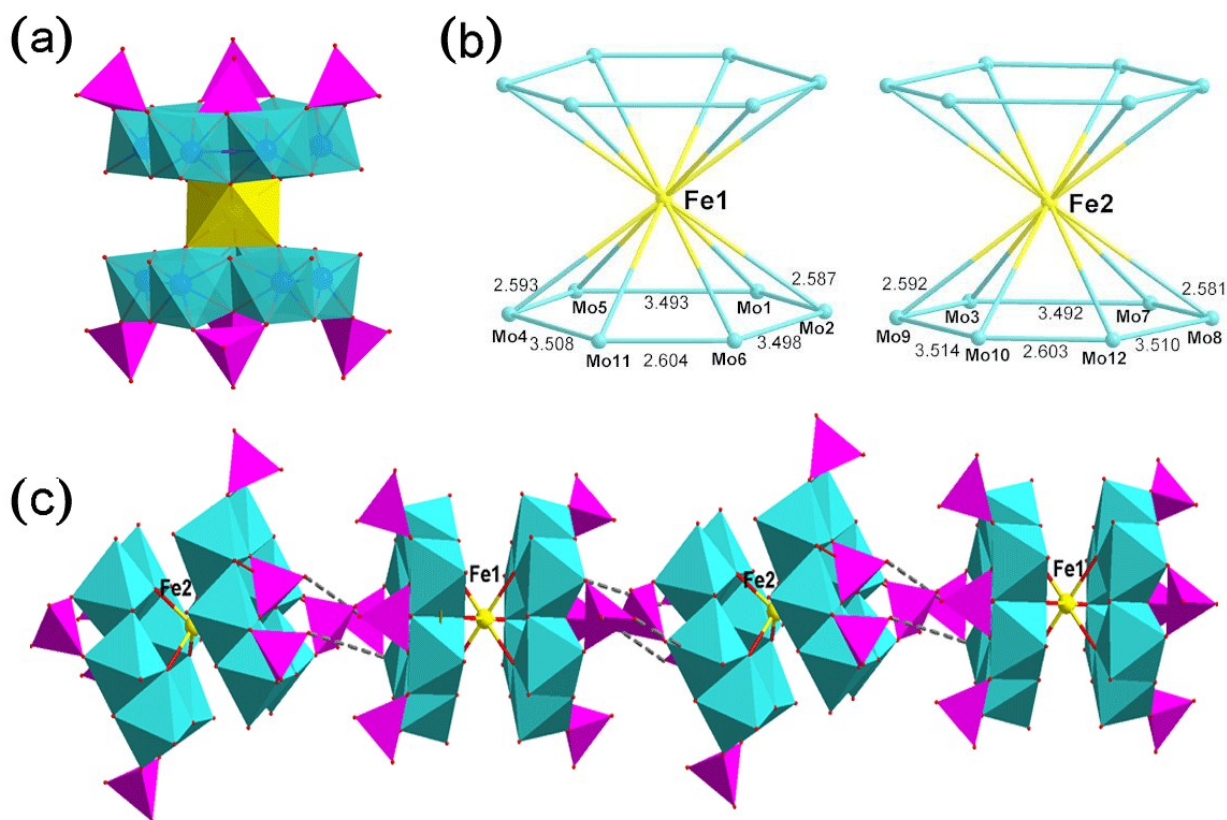


Fig. S2. (a) The polyhedral view of the sandwich type structural unit $\{\text{Fe}[\text{P}_4\text{Mo}_6]_2\}$ in **1**; (b) A simplified ball-and-rod view of two $\{\text{Fe}[\text{P}_4\text{Mo}_6]_2\}$ clusters is shown in **1**. Mo is shown as light blue, Fe atoms are yellow, and O, H and P atoms are ignored.; (c) $\text{Fe1}[\text{P}_4\text{Mo}_6]_2$ and $\text{Fe2}[\text{P}_4\text{Mo}_6]_2$ anion clusters are alternately arranged to form one-dimensional chains by hydrogen bonding.

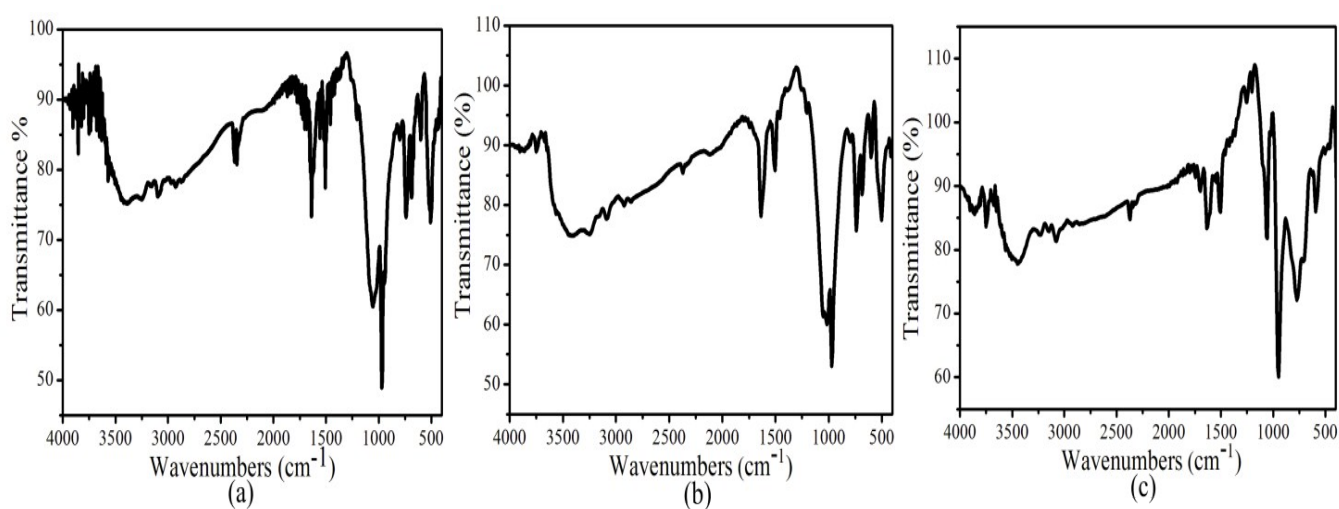


Fig. S3. IR spectra of (a) compound 1, (b) compound 2, and (c) compound 3.

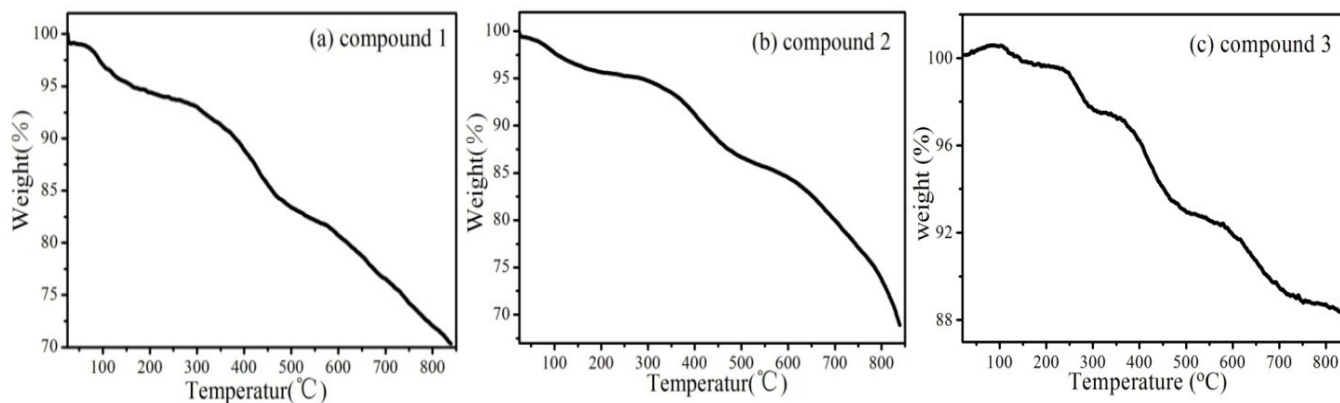


Fig. S4. TG of (a) compound 1, (b) compound 2, and (c) compound 3.

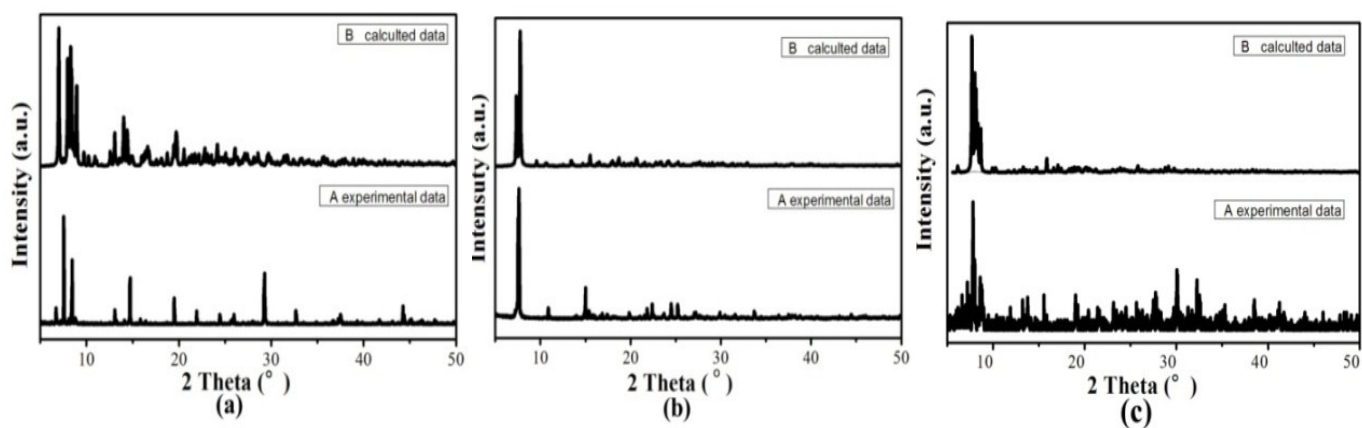
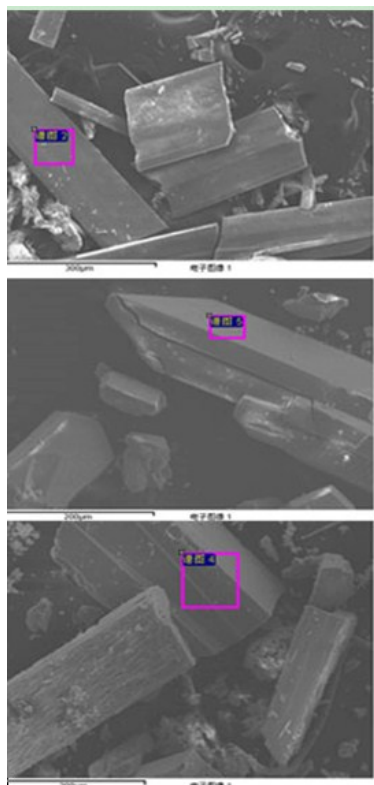


Fig. S5. Comparison of the simulated and experimental XRD patterns of compounds 1 (a), 2 (b) and 3 (c).



Elements	Weight %	atom %
1		
C K	25.37	43.75
O K	33.99	44.01
P K	7.23	4.84
Fe K	1.27	0.47
Mo L	32.14	6.94
Sum	100.00	
2		
C K	31.97	46.64
O K	42.85	46.93
P K	4.20	2.38
Zn K	2.69	0.72
Mo L	18.29	3.34
Sum	100.00	
3		
C K	29.79	49.16
O K	32.20	39.89
P K	6.65	4.25
Mn K	1.41	0.51
Mo L	29.94	6.19
Sum	100.00	

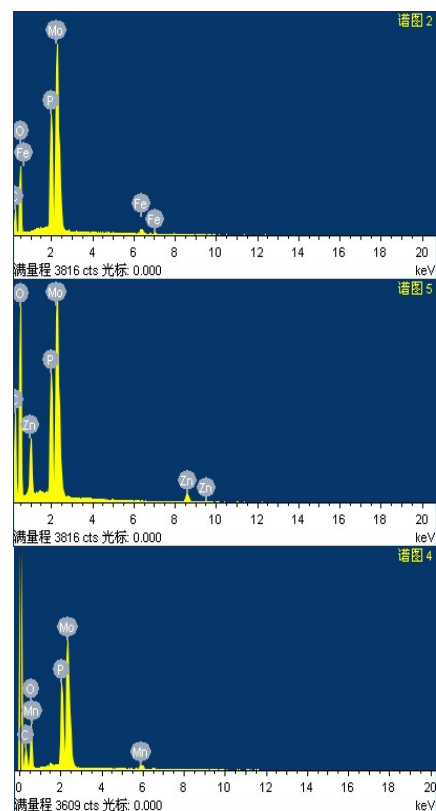


Fig. S6. EDS spectra of compounds **1-3** show the weight percentages of the elements and the total percentage of atoms. The EDS energy spectra were measured at 20 KV. The right pictures show that the compounds contain Fe, Zn, and Mn atoms. In the left Table, the atomic ratios of P:Mo:M (M = Fe/Zn/Mn) are *ca.* 4:6:1 in compounds **1-3**, and are also consistent with the structural analysis results.